SI TRACEABILITY OF FORCE AT THE NANONEWTON LEVEL

Speaker

David B. Newell
National Institute of Standards and Technology[1]
Gaithersburg, MD 20899-8112 U.S.A.
Phone: (301)975-4228 Fax: (301)975-2115 Email: david.newell@nist.gov

Paper Authors

D. B. Newell, J. R. Pratt, J. A. Kramar, D. T. Smith, L. A. Feeney, and E. R. Williams
National Institute of Standards and Technology
Gaithersburg, MD

Abstract

Although nanonewton force measurements are commonplace in industry, no National Measurement Institute supports a link to the International System of Units (SI) below one newton. The National Institute of Standards and Technology has launched a five-year inter-laboratory project focusing on the development of an instrument and laboratory capable of realizing and measuring the SI unit of force below 5 micronewtons using the electrical units as the link to the SI. We will give a brief overview of this project, instrument performance objectives and designs, and initial trials with a prototype electrostatic force balance.

Small Force Measurements

Present Status

The last decade produced a flurry of activity in the measurement of small forces. Materials scientists developed "instrumented indentation" as an indispensable tool for the study of micromechanical material properties, such as hardness and modulus(1), and for fatigue and fracture testing of thin films(2,3). Forces produced by instrumented indentation machines often range between 10^{-8} N and 10^{-2} N. Similarly, nanotechnology and biotechnology researchers adapted the Atomic Force Microscope (AFM) to quantitative force measurement, achieving 10^{-12} N resolution in studies ranging from the adhesion of ultrathin films(4) to the measurement of covalent bonds(5).

---

[1] Electricity Division, Electronics and Electrical Engineering Laboratory, Technology Administration, U.S. Department of Commerce. Official contribution of the National Institute of Standards and Technology;

In some indentation machines, these forces are calibrated to within a few percent by replacing the indentor tip with a small hook from which deadweight masses are hung[6]. According to Reference 7, calibration methods available to AFM users provide a relative uncertainty to no better than a few parts in 10^2. For example, stylus forces have been calibrated to relative uncertainties of 10^{-2} by probing an intermediary balance[8,9].

Traceability

Deadweight machines at NIST provide realizations of force from 44 N to 4.4×10^6 N with a relative accuracy of a few parts in 10^6 [10]. By applying a similar approach to small force, a deadweight load as small as 5×10^{-6} N is realized by a 0.5 mg mass, with the artifact having a relative uncertainty on the order of a few parts in 10^4 [10]. Presently NIST does not calibrate mass artifacts below 0.5 mg. In principle, there is nothing to prevent further subdivision, but the resulting artifacts will be difficult to handle. Furthermore, extrapolating the trend in small mass uncertainty[10], one expects relative uncertainties of a few parts in 10^2 in deadweights of 10^{-7} N.

A desire for accurate, traceable, small force measurement is emerging within ISO task groups and American Society for Testing and Materials (ASTM) committees working on instrumented indentation standards[11] and the fatigue and fracture of structural films. Of particular interest is the reliability of micro-electromechanical systems (MEMs)[12]. With a growing market for MEMs devices in safety critical applications, such as air bags and inertial sensors, it is time to investigate a primary force standard to provide a traceable link to the International System of Units (SI).

NIST Microforce Realization and Measurement project

In October 2000, NIST launched a five year project to develop a laboratory, measurement techniques, and instruments for the realization and measurement of forces between 10^{-8} N and 10^{-2} N. A central issue addressed by this project is the creation of a viable primary force standard below 10^{-5} N. Our goal is to realize forces on the order of 10^{-6} N and below with a relative uncertainty of parts in 10^4.

To achieve this goal, our plan is to create electrostatic forces of known magnitude and direction using a carefully designed capacitor, thereby circumventing the need for sub-milligram deadweights below 5×10^{-6} N. Traceability will be provided by an electrostatic force balance in two ways. First, the balance provides a crosscheck between electrically derived force and deadweight force, at least at the upper end of the device's useful operating range. Second, the balance allows dissemination of an electrically realized force. This is accomplished via transfer to "micro load-cells" that are calibrated against the balance using procedures analogous to those described in References 8 and 9.

Electrostatic Force Balance

Principle

The mechanical work required to change the separation between the two electrodes of a capacitor while maintaining a constant voltage is:

$$dW = Fdz = \frac{1}{2}V^2 dC \qquad \text{Eq. 1}$$

where dW is the change in energy, F the mechanical force, dz the change in separation, V the voltage, and dC the change in capacitance. Thus a mechanical force can be related to the electrical units by measuring the voltage applied across a capacitor and the capacitance gradient, dC/dz:

$$F = \frac{1}{2}V^2 \frac{dC}{dz} \qquad \text{Eq. 2}$$

Balance Design Constraints and Possible Accuracy

An electrostatic force can be compared to a deadweight force by monitoring the change in voltage necessary to keep the separation of the capacitor electrodes constant when a mass standard is added to the "freely moving" electrode. To keep the comparison uncertainty below a few parts in 10^5, the "freely moving" electrode travel axis must be aligned with respect to gravity to 10 mrad. Furthermore, the restoring force of the electrode support structure must be sufficiently smaller than the applied force for an observable deflection.

The capacitor geometry can be optimized for a more accurate determination of dC/dz. The capacitance per unit length of two infinitely long concentric cylinders is a constant. This geometry can be closely approximated by a long cylindrical electrode, inside and concentric with another long cylindrical electrode, and appropriate shielding such that the fringing fields remain constant when there is a relative displacement along the symmetry axis. This improves the determination of dC/dz over a relatively large range.

Assuming a value of dC/dz=1 pF/mm, an application of 1 V across the capacitor results in a force of 5×10^{-10} N, while application of 1000 V yields a force of 5×10^{-4} N. Voltages of these magnitudes are easily produced and measured, with relative uncertainties of a few parts in 10^6. Picofarad capacitance levels can be measured with the best commercial bridges to a relative uncertainty of a few parts in 10^6, while the best commercial differential-displacement interferometers can accurately measure translations on the order of 10^{-9} m, provided there is adequate environmental control. This displacement resolution limits the effective spring constant of the moving electrode support structure to < 1 N/m to resolve 10^{-9} N. By measuring the capacitance as a function of displacement over an interval of 1 mm, we may achieve relative uncertainties on the order of a few parts in 10^6 in our determination of dC/dz. This would imply an SI determination of a 5×10^{-10} N force with an uncertainty on the order of 10^{-14} N. We now describe our first attempt to realize these parameters.

Experiment

Apparatus

While early work with equal arm balances proved promising due to the very weak restoring force of the support structure, a spring balance was used for initial results due to the constrained motion in a known direction. A schematic of the spring balance is shown in Figure 1. It features a compound-rectilinear leaf spring that suspends and guides the motion of a 2 mm diameter, 46 mm long glass rod. The top of the glass rod protrudes from the spring assembly and forms the balance platen. Fitted to the bottom of this rod is the inner electrode. The inner electrode is an inverted, thin-walled cylindrical cup, high-speed milled from 6061-T6 Aluminum, with a 15 mm diameter, 15 mm length, and a wall thickness of 0.25 mm. The inside floor of the cup is diamond turned to produce the measurement mirror surface for the double-pass Michelson heterodyne interferometer. This entire assembly mounts to a 5-axis stage for fine positioning of the device with respect to the outer electrode, and for alignment of the motion axis to gravity. The outer electrode is 90 mm long, with a 44.5 mm diameter and a 15.9 mm diamond turned bore through the center. The bottom face of this cylinder is diamond turned orthogonal to the bore in a single setup to produce the surface of the reference mirror. The outer electrode is held in a tip-tilt laser mount to facilitate alignment of the interferometer. Capacitance per unit length is calculated as $dC/dz = 0.98$ pF/mm, assuming a pair of infinite concentric cylinders.

Alignment procedure

The vertical translation stage of the inner electrode was characterized, aligned with respect to gravity, and used as a transfer standard to align the spring flexure travel axis. The alignment procedure is synchronous with the assembly of the experiment. First a reference laser beam was aligned to 1 mrad with respect to gravity using a flat and a precision bubble level. A quadrant photo-detector was then mounted on the vertical translation stage to detect horizontal motions. The vertical translation stage was moved using a motorized-micrometer screw and was initially characterized over a range of 2 mm. Large scale horizontal motions of the stage were reduced by adjusting the angle of the stage. Periodic horizontal motion of 0.5 mm was detected due to the screw rotation, so an intervening motion decoupling stage was installed. The stage travel had deviations of 3 µm, but a vertical travel range of 0.7 mm was identified as having residual horizontal motion less than of 0.35 µm, corresponding to a misalignment of 0.5 mrad with respect to the laser beam.

The inner electrode was mounted on the vertical translation stage at the same position where the quadrant photo-detector had characterized the horizontal motion. The outer electrode was installed such that the inner electrode was completely inside. It was also displaced horizontally such that one side was as close as possible to the outer electrode. This offset allows the detection of horizontal motion through the horizontal capacitance gradient that was roughly 0.2 pF/µm at a

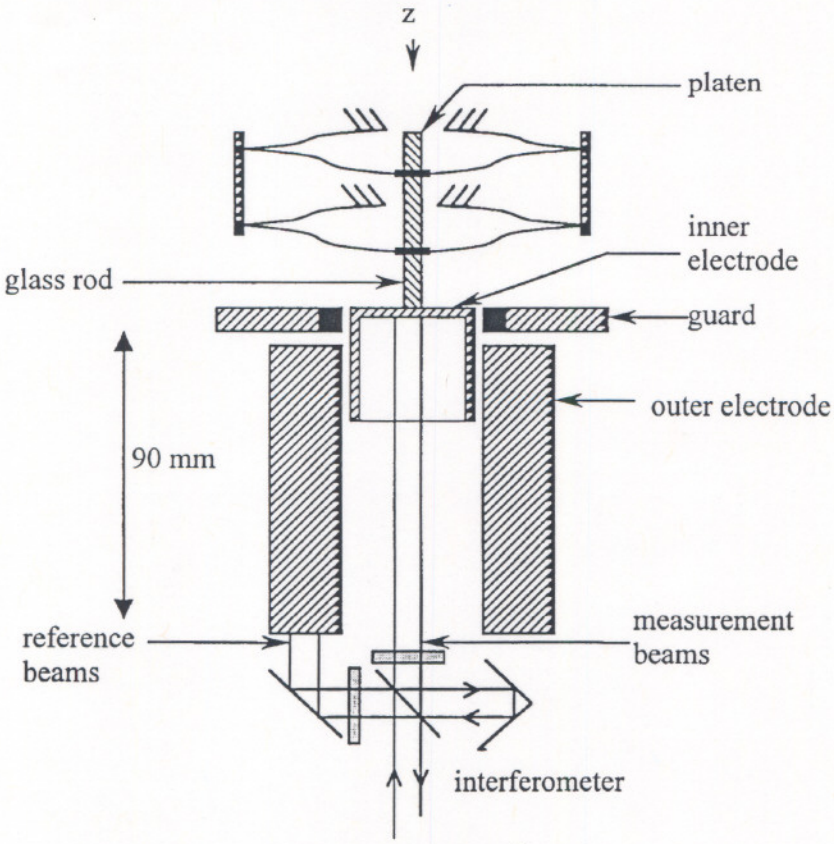

Figure 1: Schematic of an electrostatic spring balance.

capacitance of 25 pF. The vertical stage was moved over the identified range while the inner electrode was held vertically motionless by a small probe contacting the platen. The observed horizontal motion was then reduced by tilting the spring flexure travel axis. The inner electrode was placed near the outer electrode at four positions to align both tilts. We estimate the final overall uncertainty of the flexure travel axis with respect to gravity to be 2 mrad.

Capacitance Gradient Measurement

The capacitance gradient was measured with a nominal vertical overlap between the two electrodes of 5 mm. The inner electrode was horizontally centered inside the outer electrode by translating the outer electrode and minimizing the capacitance. Once the balance was placed inside an electrostatic shield, the measurement process was totally automated. The inner electrode was displaced vertically by pushing on the platen with a small probe connected to a motorized translation stage. The stage was repeatedly moved up and down over a selected range and step size. At each position the interferometer reading and capacitance were averaged for 1 second and recorded.

Initial measurements made over a 0.7 mm range at 0.1 mm steps showed a nonlinear dependence in dC/dz due to the finite lengths of the electrodes and the changing fringing electric fields. Tests for changing stray capacitance were performed by adding a 100 pF capacitor between an electrode and ground, producing an apparent change in the capacitance gradient of no more than a part in 10^4. Alignment tests were also performed by comparing dC/dz values obtained from moving the inner electrode along its flexure travel axis to values obtained by moving its translation stage. The agreement was within a part in 10^4.

It is important to determine dC/dz at the force comparison position. A specific range of ±0.1 mm (centered around the weighing position) with a step size of 0.01 mm was selected. Measurements were completed over 100 minutes, producing over 1700 capacitance/position values. Single dC/dz values were calculated for each single round trip up/down scan to reduce the effect of linear drift in the measurement. These are plotted in Figure 2a) against the average position of the scan as determined by the interferometer reading. The actual average position of a single up/down scan varied due to creep and missing steps of the motorized-micrometer. A linear fit of dC/dz as a function of position was used to determine a value of $dC/dz = 0.94466 \pm 0.00005$ pF/mm (standard deviation of the residuals) at the weighing position. The residuals formed by subtracting the fit from the individual dC/dz values plotted against the start time of each scan produce an upper limit estimate of the drift of dC/dz of 2 parts in 10^4/day and are shown in Figure 2b). These results are consistent with a previous test of two similar measurements separated by 48 hours but made over the same 0.12 mm range as measured by the interferometer. These reproduced the same value for dC/dz to within parts in 10^4. The remaining scatter in Figure 2b) is most likely due to pressure and temperature changes effecting the dielectric constant and refractive index of air, which are estimated to be of the order of parts in 10^4.

A second analysis was performed by selecting all the capacitance and position measurement pairs that were centered around the weighing position as determined by the capacitance measurement. After removing the linear trend of capacitance as a function of position, the residuals were plotted against time, showing a nonlinear drift of roughly 0.0003 pF over 100 minutes. An estimate of the capacitance correction as a function of time was achieved by applying a third order fit. A linear fit was then used on the corrected capacitance and position pairs, yielding $dC/dz = 0.944619 \pm 0.000014$ pF/mm (standard deviation of the residuals).

The precise determination of the spring constant, k, of the compound-rectilinear leaf spring is not important for comparing a deadweight force with an electrically derived force if the balance is operated in a null mode. However it is still informative and useful to compare forces as determined by using a spring constant and a measured deflection. The spring constant of the compound-rectilinear leaf spring was determined by applying a voltage across the electrodes in 10 V steps from 0 to 1000 V, measuring the corresponding displacement, and using the experimentally determined value of dC/dz. The voltage was ramped up and down four times with the voltage and interferometer reading being averaged over 1.6 seconds at each position. A value of k was calculated between each 10 volt step, resulting in an average value of $k = 13.42 \pm 0.64$ N/m (standard deviation uncertainty).

Force Measurements

The force resolution of the balance was determined by repeatedly applying a voltage of 0 and 10 V across the electrodes with the position being measured as described above. To eliminate offsets and reduce the effect of linear drift, the apparent deflection was determined by the difference between the interferometer reading at a 0 (10) V measurement and an average of the two adjacent 10 (0) V measurements. The voltage was alternated 140 times. The resulting deflection was $(3.3 \pm 1.8)\times10^{-9}$ m, which corresponds to a force of 47×10^{-9} N using dC/dz and the voltage applied, and a force of 44×10^{-9} N using the calculated spring constant. This is the limit of our force resolution using this spring balance and interferometer.

A deadweight force and an electrically derived force were compared using a 5 mg mass standard. Once a bias voltage of roughly 700 volts was applied across the electrodes, the position was recorded and defined as the "weighing" position, the measurement process was totally automated. The 5 mg mass standard was placed on and removed from the platen using the motorized translation stage. During a mass exchange, the position of the platen (and inner electrode) was held constant by feeding back the interferometer reading to the voltage being applied to the electrodes. The temporary deflection was less than 3 μm during the exchange, with the change in voltage of roughly 75 V. After each mass exchange, the voltage was integrated for 3.3 seconds. Again, to eliminate offsets and reduce the effect of linear drifts, the electrically derived force was determined by the difference between the voltage with the mass on (off) and an average of the two adjacent mass off (on) voltage measurements. A total of 32 weighings were performed. The resulting calculated electrical force yields $(48.841 \pm 0.051)\times10^{-6}$ N (standard deviation uncertainty). The mass artifact was calibrated to be 5.00085 ± 0.00027 mg. By using a value of 9.80103 ± 0.00001 m/s^2 for gravity as determined by a nearby absolute gravimeter and applying a buoyancy correction, the mechanical force is calculated to be $(48.9921 \pm 0.0026)\times10^{-6}$ N. The comparison between the electrical and mechanical force yields a discrepancy of 3×10^{-3}.

Uncertainty Discussion

Uncertainties are divided into Type A and Type B as discussed in Reference 13. Type A uncertainties of the electrically derived force can be taken as the standard deviation listed above. While there may be other type B uncertainties, such as a systematic effect due to the flexure hysteresis, only uncertainties due to the measurement of the three quantities (length, capacitance, and voltage) will be considered here.

The uncertainties in the wavelength and stability of the laser are relatively insignificant. The path-length difference between the two interferometer arms was 0.1 m. After correcting for the index of refraction using Edlen's formula at standard temperature, pressure, and humidity, and assuming the pressure and temperature do not change by more than 1% during the time it takes for a single ±0.1 mm scan (roughly a few minutes), an uncertainty of 5×10^{-5} can be assigned to dC/dz due to the change of the optical path length. There was a 5 ± 0.3 mrad measured cosine error due to the angle of the mirrored surface of the inner electrode. A correction was applied to the value of dC/dz, with a resulting total uncertainty (including alignment with respect to vertical) of 2×10^{-6}. The combined Type B relative uncertainty for the length measurement is 5×10^{-5}.

For the capacitance measurement, a generous estimate of the relative uncertainty due to the selected capacitance bridge and standard is 10^{-5}. The correction due to dielectric constant of air is 6×10^{-4}. Assuming the pressure and temperature do not change by 10% between a *dC/dz* determination and a force comparison (roughly a few days for this particular comparison), the uncertainty due to the changing dielectric constant of air is on the order of 6×10^{-5}. Stray capacitance effects are described in the capacitance gradient measurement section and assigned a relative uncertainty of 1×10^{-5}. The combined Type B relative uncertainty for the capacitance measurement is therefore 6.1×10^{-5}.

An estimate of the relative voltage uncertainty from the DVM manufacturer's specification at this range of voltages is on the order of 10^{-5}. This appears twice in the force measurement. The AC voltage from the high voltage power supply used was measured to be 0.02 V over a 10 MHz bandwidth at an operating voltage of 700 V corresponding to a systematic force error of 10^{-14} N. The combined Type B relative uncertainty for the voltage measurement is 2.8×10^{-5}.

By adding the individual Type B uncertainties in quadrature, the total Type B relative uncertainty due to length, capacitance, and voltage measurements is 8×10^{-5}. However as noted above, this is not a complete analysis of systematic errors. There is an uncertainty in the value of *dC/dz* used to perform a weighing due to lack of environmental control. This value will change due to the dielectric constant, and the measured weighing position will change due to the refractive index of air. Work is continuing on providing a history of alternating *dC/dz* determinations and weighings while monitoring pressure and temperature. To get a better uncertainty estimate due to the linearity of the electrically derived force, work is also continuing on providing force comparison using 1 and 20 mg mass standards.

Future of the project

Transfer standards

For dissemination transfer standards are required that can be calibrated and shipped. We plan to begin examining possible transfer standards in the coming year. Two examples are a cantilever capacitor, similar to the one demonstrated in Reference 10, and a commercially available piezoresistive AFM cantilever. In principle, these artifacts can be calibrated against the primary balance to determine their voltage output at various force levels. A key challenge in the dissemination will be providing clear instructions to the end user describing the axis along which the force is to be applied.

Laboratory

A nested room within a room is under construction to provide a clean environment with electric, acoustic, and vibration isolation. An electrically shielded, acoustic isolation chamber nominally 2.4 m x 2.4 m x 5 m will house a vibration isolated optical table on which experiments can be set up and performed. Heating, ventilation, and cooling air will be supplied to this room through two baffled silencer systems that terminate in filters located on the ceiling of the room. Air will exhaust at the base of the room around its perimeter to create a so-called laminar flow environment. Temperature, pressure, and humidity will be monitored and controlled within the shielded chamber, though it is anticipated that the experiments will eventually be performed within a small bell jar at modest vacuum and that temperature will be controlled locally. Entry to the shielded room will require passage through a nominal class 1000 clean room environment that incorporates a pass-through box for transferring specimens (e.g., micro-load cells) from a sample preparation and inspection area immediately adjacent.

References

(1) Oliver, W. C. and Pharr, G. M., "An improved technique for determining hardness and elastic modulus using load and displacement sensing indentation experiments," J. Mater. Res, 77:6, 1992, pp. 1564-1583.

(2) Wu, T. W., Shull, A. L., and Berriche, R., "Microindentation fatigue tests on submicron carbon films," Surface and Coatings Technology, 47, 1991, pp. 696-709.

(3) Kriese, M. D., Boismier, D. A., Moody, N. R., and Gerberich, W. W., "Nanomechanical fracture-testing of thin films," Engineering Fracture Mechanics, 61, 1998, pp. 1-20.

(4) Umemura, S., Hirono, S., Yasuko, A., and Kaneko, R., "Wear Durability and Adhesion Evaluation Methods for Ultrathin Overcoat Films by Atomic Force Microscopy," IEICE Trans. Electron., E81-C:3, 1998, pp. 337-341.

(5) Grandbois, M., Beyer, M., Rief, M., Clausen-Schaumann, H., and Gaub, H., "How Strong is a Covalent Bond?," Science, 283:12, 1999, pp. 1727-1730.

(6) MTS Nano Instruments Innovation Center Nano Indenter II Calibration Instructions, Version 1.0

(7) Howard, L. P. and Fu, J., "Accurate force measurements for miniature mechanical systems: a review of progress," SPIE Proceedings Series, 3225, 1997, pp. 2-11.

(8) Hoffman, W., Loheide, S., Kleine-Besten, T., Brand, U., and Schlachetzki, A., "Methods of characterising micro mechanical beams and its calibration for the application in micro force measurement systems," MICRO.tec 2000, 2000, Hannover.

(9) Smith, S. T. and Howard, L. P., "A precision, low-force balance and its application to atomic force microscope probe calibration," Rev. Sci. Instrum., 65:4, 1994, pp. 903-909.

(10) Jabbour, Z. L., and Yaniv, S. L., "The Kilogram and the measurements of mass and force," Journal of Research of the National Institute of Standards and Technology, 106, 2001, pp. 25-46.

(11) ISO group TC 164/SC 3/WG 1 and ASTM E28.06.11, see for instance ISO/DIS 14577-1, 2 and 3.

(12) Symposium on Mechanical Properties of Structural Films, November 15-16, 2000, Orlando, Fla, sponsored by ASTM E08, Christopher Muhlstein, UC Berkeley, Chairman.

(13) Taylor, B. N. and Kuyatt, C. E., "Guidelines for Evaluating and Expressing the Uncertainty of NIST Measurement Results," NIST Tech. Note 1297, 1994.